Proceedings of the ASME 27th International Conference on Offshore Mechanics and Arctic Engineering
OMAE2008
June 15-20, 2008, Estoril, Portugal

OMAE2008-57459

MODELING AND SIMULATION OF AN UNDERWATER REMOTELY OPERATED VEHICLE (ROV) FOR SURVEILLANCE AND INSPECTION OF PORT FACILITIES USING CFD TOOLS

Raúl A. Valencia*
Universidad Pontificia Bolivariana
Department of Mechanical Engineering
P.O. Box 56006
Medellín, Colombia
telephone: 574-415-9020
fax: 574-411-8779
raul.valencia@upb.edu.co

Juan A. Ramírez
Universidad Pontificia Bolivariana
Department of Mechanical Engineering
P.O. Box 56006
Medellín, Colombia
telephone: 574-415-9020
fax: 574-411-8779
juan.ramirez@upb.edu.co

Luis B. Gutiérrez
Universidad Pontificia Bolivariana
Department of Electrical and Electronics Engineering
P.O. Box 56006
Medellín, Colombia
telephone: 574-415-9020
fax: 574-411-8779
luis.gutierrez@upb.edu.co

Manuel J. García
Universidad EAFIT
Department of Mechanical Engineering
P.O. Box 3300
Medellín, Colombia
telephone: 574-261-9500
fax: 574-266-4284
mgarcia@eafit.edu.co

ABSTRACT

This article presents theoretical and computational studies with Computational Fluids Dynamics (CFD) tools of an Underwater Remotely Operated Vehicle (ROV), required to obtain reliable visual information, used for surveillance and maintenance of ship shells and underwater structures of Colombian port facilities. The thrust force is analyzed at the operational conditions by using CFD tools (FLUENT^{TM}, CFX^{TM}, COSMOSFLOW^{TM}) and the information about forces, torques and power of the vehicle's thrusters is obtained. The commercial propellers were modeled by using a reverse engineering process with a 3D scanner and Computer Aided Design (CAD) software (RAPIDFORM^{TM}). The results obtained with the CFD package allowed to evaluate several operating scenarios of the vehicle that are used for feedback purposes in the design process of the ROV before it be manufactured.

Keywords: Propulsion, ROV, CFD, Reynolds Averaged Navier Stokes solver, CFX.

INTRODUCTION

The remotely operated underwater vehicles (ROVs) have had a wide development in industrialized countries and a great amount of experiences at the industrial, commercial, and academic levels. It's possible to find applications such as maintenance and sea operations in the oil industry, military applica-

*Address all correspondence to this author.

tions (monitoring, recognition), inspection and maintenance for the port industry and underwater research. Three categories for this kind of vehicles can be defined: heavy work, observation and mini/micro ROV [1].

The operation sites of the vehicle are the most important commercial interchange seaports of Colombia: Cartagena, Barranquilla, Santa Marta and Buenaventura. These locations define the operational conditions: depth, density, salinity, temperature and stream parameters. Among the water characteristics related to the problem to be solved, we find: low compressibility, heating capacity and thermal conductivity, sea water density varies depending on the depth, the temperature and the salinity. In terms of the temperature, the water takes a maximum density of about 4°C. In terms of salinity, it produces an increase in the density. In terms of depth, the density of sea water varies from 1012 kg/m^3 in the surface to 1070 kg/m^3 at 1000 m deep. The temperature varies depending on the depth of the zone; between 0 and 200 m deep, the temperature is very similar to the surface one and it approaches 0°C when the depth increases to more than 4000 m [2].

In the design process of an ROV it's necessary to know all the possible disturbances that affect its movement and write them in terms of relations that allow a better performance of the control system. Therefore, an appropriate study of the propulsion system helped to guarantee an accurate and stable positioning of the vehicle. In order to accomplish this, it is important to know the exact relation between the engine's power (or other variables, such as the voltage or the motor's torque) and the thrust that is provided by each propeller. Such expression is defined by the action of the motors and the performance of propellers. The relation between the power and the thrust is useful for the hydrodynamic study of the propellers and other elements of the propulsion system that interact with the fluid.

The vehicle's operation depth defined for 100 m, which corresponds to a hydrostatic pressure of 1.00 MPa (145.5 psi), although, one of the objectives of the vehicle is the inspection in Colombian ports, where the following depths appear according to reports of the Regional Port Societies of Colombia.

Port	Maximum depth (m)
Barranquilla	12.0
Buenaventura	13.7
Cartagena	13.7
Santa Marta	18.3

Table 1. Colombian ports depth

The vehicle's operation speed depends on the stream speed under which it will be operating in the designated locations (ports), with the purpose of guaranteeing that the submersible has the capacity to stay static despite their direct incidence on it. Due to the current conditions in the ports, a terminal maximum operational speed of 1.5 m/s is defined.

PHYSICAL MODEL

Loads of interest

The loads that influence the behavior of the vehicle are [3]:

- Weight: gravitational force
- Displacement: force due to the vertical pressure gradient (weight of the displaced volume)
- Drag and lift: loads due to the relative motion between the vehicle and the water.
- Thrust: forces generated as a reaction to the rate of change of the angular and linear momentum of fluid particles.
- Contact forces: contacts with objects, waves, and wind.
- Inertial loads: due to vehicle changes in linear and angular momentum.

The propeller

The propeller transforms most part of the input power into thrust force [3, 4]. They're usually moved by electrical motors. The parts of a propeller are shown in figure 1.

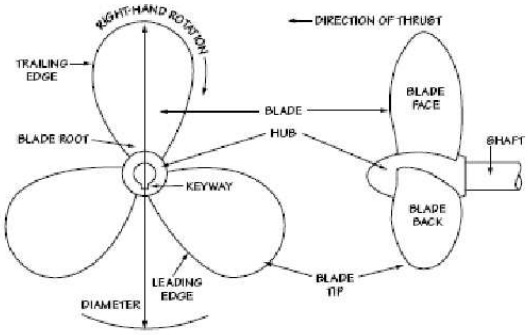

Figure 1. Parts of a propeller

Where:

- D: diameter of the propeller
- Hub: central part of the propeller which supports the blades.
- Blade tip point: the farthest point of the blade measured from the hub axis.
- Blade root: place in wich the blades are attached to the hub.
- Tip circle: circle described by the tips when the propeller rotates.

- Propeller disc area: area of the circle framed by the tip circle trajectory.
- Leading edge
- Training edge
- Pressure face: side of the propeller blade that has the greatest pressure in an advancement movement
- Suction back: low pressure side of the blade.
- *P*: Pitch

The first objective is to evaluate, by using CFD tools, the performance of a commercial propeller with the following specifications:

- Brand: Harbor Models
- Material: Bronze
- Diameter: 0.0889 m
- Pitch: 0.1016 m
- Rotation: right
- Number of blades: 4

Figure 2 shows a picture of one of these propellers. Figure 3

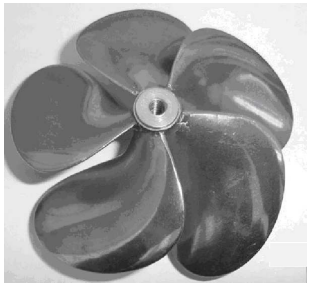

Figure 2. Propeller Harbor Models(5 blades)

shows a simplified CAD model of the propeller and the kort nozzle assembly. The thrust force produced by the propeller and

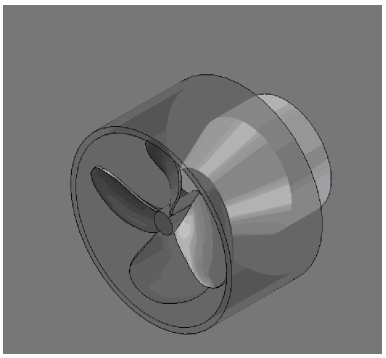

Figure 3. Simplified CAD model

transfered to the water, varies due to inefficiencies of the propeller, the motor-reductor set, the drive shaft assembly and the sealing systems. In spite of the thrust variations, the vehicle must reach enough speed to overcome drag and sea streams.

There are two kinds of thrust forces: static and dynamic [5]. The first one is refered to the power applied to the propeller when the vehicle doesn't move, this happens in tests made in tanks or pools. The second applies when the vehicle moves and inertia and momentum must be considered.

MATHEMATICAL MODEL

The calculations were made using the Ansys-CFX program. The model equations are the Reynolds-averaged Navier-Stokes (RANS) equations [6].

$$\frac{\partial \rho}{\partial t} + \frac{\partial}{\partial x_i}(\rho u_i) = 0 \quad (1)$$

$$\frac{\partial(\rho u_i)}{\partial t} + \frac{\partial(\rho u_i u_j)}{\partial x_j} = -\frac{\partial p}{\partial x_i} + \frac{\partial}{\partial x_j}\left[\mu\left(\frac{\partial u_i}{\partial x_j} + \frac{\partial}{\partial x_i} - \frac{2}{3}\delta_{ij}\frac{\partial u_i}{\partial x_l}\right)\right] + \frac{\partial}{\partial x_j}\left(-\rho\overline{u_i' u_j'}\right) \quad (2)$$

where δ_{ij} is Kronecker's delta and $\left(-\rho\overline{u_i' u_j'}\right)$ are Reynolds' stresses. Two turbulence models used in hydrodynamics and applications of engineering to predict the characteristics of rotating flows are $k-\omega$ and Reynolds' transport stresses (RTSM), the second one is the most commonly used. In this particular case the turbulence is considered because the inertial forces of the fluid are significant compared to the viscous forces. The RTSM is used because of its good predictions in this kind of problems. In general, the turbulence model modifies Navier-Stokes equations for the introduction of the average and the fluctuating amounts that produce the average equations of Reynolds Navier-Stokes (RANS). The model of turbulence used was the Shear Stress Transport Model (SST) based on the $k-\omega$ model. It considers the transport of the sharp turbulence stresses and gives a good prediction of the flow separation under pressure gradients [7].

With respect to the action of the propeller, when a propeller rotates it creates a high pressure zone in the front area and a low pressure zone in the back part [4]. The water goes from the high to the low pressure zone creating a differential of pressure and force to the vehicle. Basically, there are three theories that deal with the action of the propeller: the momentum theory, the propeller blade section theory, and the circulation theory.

Experimental information on different propeller families is available in curves resulting from open flow tests. The parame-

ters of these curves are [4]:

$$J = \frac{2\pi V_A}{\omega D} \tag{3}$$

$$K_T = \frac{4\pi^2 S}{\rho\omega^2 D^4} \tag{4}$$

$$K_Q = \frac{4\pi^2 Q}{\rho\omega^2 D^5} \tag{5}$$

$$\eta_0 = \frac{J}{2\pi}\frac{K_T}{K_Q} \tag{6}$$

Where:

- J: advance ratio
- K_T: thrust coefficient
- K_Q: torque coefficient
- η_0: propeller efficiency

Other important expressions are:

$$\eta_t = \eta_d \sqrt{\frac{\rho\pi}{4}}\frac{D}{\sqrt{S}} \tag{7}$$

$$\eta_t = \frac{K_T}{K_Q}\frac{1}{\omega D} \tag{8}$$

$$\eta_d = \frac{(\frac{K_T}{\pi})^{\frac{2}{3}}}{K_Q} \tag{9}$$

The torque, speed and required power to move the propeller are given by:

$$\omega = \frac{2}{\sqrt{\rho}}\sqrt{\frac{S}{K_T}\frac{1}{D^2}} \tag{10}$$

$$Q = \frac{P}{\omega} = \frac{K_Q}{K_T} SD \tag{11}$$

$$P = \frac{1}{\eta_d}\sqrt{\frac{4}{\rho\pi}\frac{S^{\frac{3}{2}}}{D}} = \frac{2\pi}{\sqrt{\rho}}\frac{K_Q}{K_T^{\frac{3}{2}}}\frac{S^{\frac{3}{2}}}{D} \tag{12}$$

The effect of the parameters given by (3) to (12) have been experimentally analyzed for a wide family of propellers. This family of propellers is the Wageningen B-series [8], the notation used is B.5.60 where the number 5 indicates the number of blades (z) and the 0.60 indicates the area of action of the propeller ($AE/A0$). A typical curve of this family of propellers is shown in figure 4.

In the propeller selection problem there are six unknown variables: thrust (T) or drag (R), the speed of advancement (V_A), pitch (P), diameter (D), rpm (n), torque (Q). Four of these unknown variables must be known in order to apply (3) to (12)

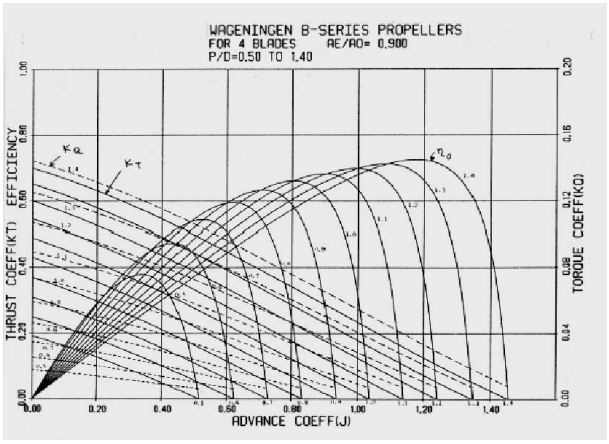

Figure 4. Typical curve of the family of Wageningen propellers. Source: BERNITSAS, M.; RAY, D. y KINLEY, P. KT, KQ and efficiency curves for the Wageningen B-series propellers. Department of Naval Architecture and Marine Engineering. University of Michigan.

and solve the selection problem. For example, if the drag (R) is known, the revolutions (n) based on the selection of the motor, the diameter of the propeller and the velocity, K_T and J can be calculated from (3) to (12), defining a point in the K_T-J curve. The P/D curve that goes through the point, determines the pitch (P) and the corresponding value for K_Q from which the torque (Q) can be calculated. Once these parameters are found, the delivered power can be calculated though the following equation:

$$P_D = \frac{2\pi\omega Q_0}{\eta_R} \tag{13}$$

For the analysis of transitory flow and in the calculation of the time increase, the Courant Number was taken into consideration and it was defined for one dimension:

$$C = \frac{u\Delta t}{\Delta x} \tag{14}$$

where the velocity of the flow is u, the time increase is Δt and the size of the mesh is Δx.

Some of the simplifications that were taken into consideration were:

- The flow is considered incompressible.
- The flow is turbulent modeled by RANS mimicing the effects of turbulence in a Newtonian fluid to determine the time-averaged or slowly varying flow around a propeller.
- The axis of the propeller rotates at constant angular velocity and the velocity of advancement is constant.

- The blade surface with a relative roughness of zero (ideally smooth).

SOLUTION STRATEGY

To solve the problem two domains were defined: a stationary domain that covers the open flow and propeller's knort nozzle and motor zone; and a domain that covers the zone were the propeller rotates [7] (figures 5 and 6).

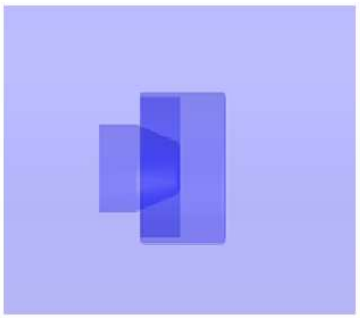

Figure 5. Stationary domain

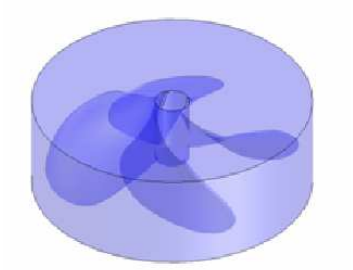

Figure 6. Rotating domain

Through CAD boolean operations (using Solid Edge^{TM}), the motor, protector and propeller's geometries were subtracted from the domains such that only the zone of the fluid remain in the model. The propeller's CAD model was generated through an inverse engineering process, where a series of refinements were made from the cloud point to the generation of the surfaces and the later construction of the virtual model. The programs used were: Rapidform^{TM}, Rhinoceros^{TM} and Solid Edge^{TM}. Figure 7 illustrates the process.

The mesh was generated through ANSYS^{TM} ICEM, in which the domains were meshed with unstructured meshes using tetrahederal elements. The propeller's mesh was more refined to

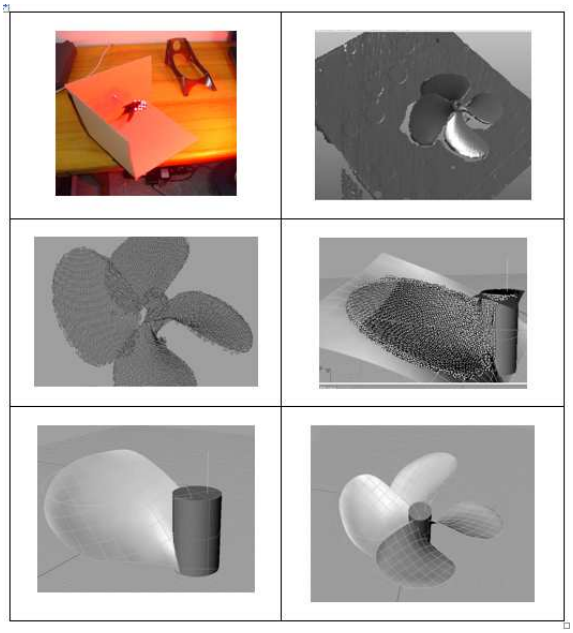

Figure 7. Inverse engineering of the propeller

observe in detail flow's behavior in the root, surface and the edge of the blade. The mesh of the stationary domain was defined with bigger elements in the open fluid zone. The motor and protector zone was refined with smaller elements (figure 8).

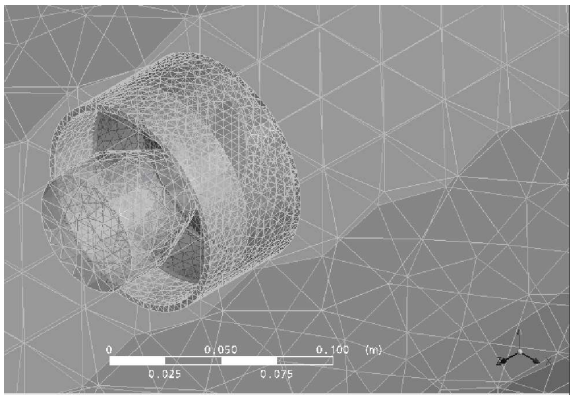

Figure 8. Mesh of the domains in ANSYS ICEM

Some simplifications were made in the geometry of the model (Figure 3), before the mesh was created: elimination of holes, rounds and fillets, also an average blade thickness was used. The number of nodes and elements of the domain are presented in table 2.

The size of the open flow domain was defined based on the diameter of the propeller according to the guidelines of [9] that

Domain	Nodes	Elements
Openwater (estacionary)	18131	94113
Propeller (rotating)	14309	73225
Total	32440	167338

Table 2. Mesh information

not affect the boundary conditions: five times the diameter upstream and ten times the diameter downstream for observing the development of the wake generated by the propeller. The domain was radially increased four times in order to observe the flow's behavior through the external side of the protector. It was oriented so that the *z* axis coincides with the propeller axis (figure 9).

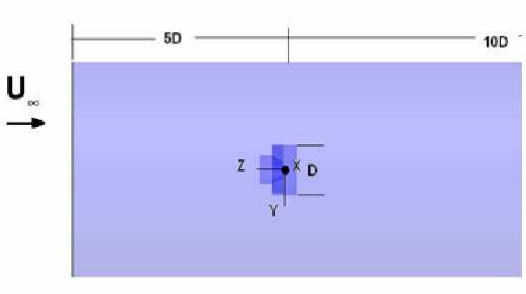

Figure 9. Size of the open flow domain

The specifications applied in the pre-processing stage are shown on table 3).

Domain	Specifications
Stationary	Name: openwater
Rotating	Name: propeller
Turbulent Model	SST (shear stress transport)
Fluid	Water

Table 3. Boundary conditions defined in ANSYS

In the post-processing stage, new variables based on the propeller's mathematical model were created in order to monitor convergence and to analyze propeller's performance. Some of the variables were: advance ratio (J), thrust coefficient (K_T), torque coefficient (K_Q), power, thrust and torque.

The first analysis was made in steady state and these results were used in the transitory state as initial conditions. The scheme of solution employed with ANSYS-CFX was *High Resolution* with a number of initial iterations of 100. But after observing the convergence curves at 50 iterations, it was possible to have good stability in the solution. After the post-processing was made, it was possible to obtain graphs showing the behavior of pressures, pathlines, speed vectors, among others. The CPU time was 31.35547 minutes with a computer of 3.00GHz and 1.00GB de RAM.

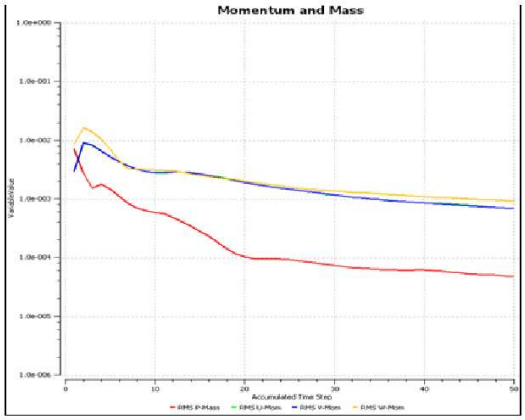

Figure 10. Momentum and mass

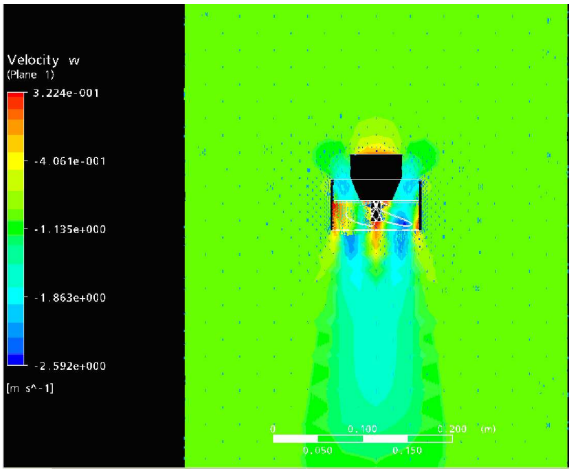

Figure 11. Velocity *w* profile

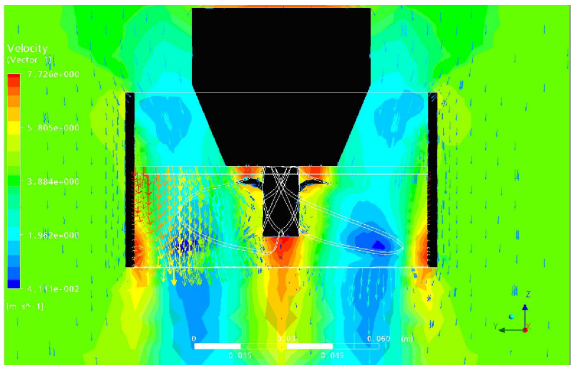

Figure 12. Velocity vectors

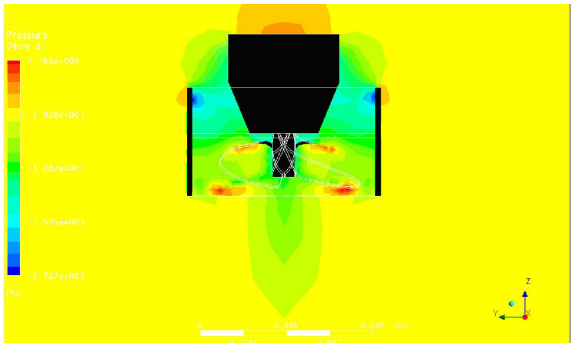

Figure 13. Pressure distribution

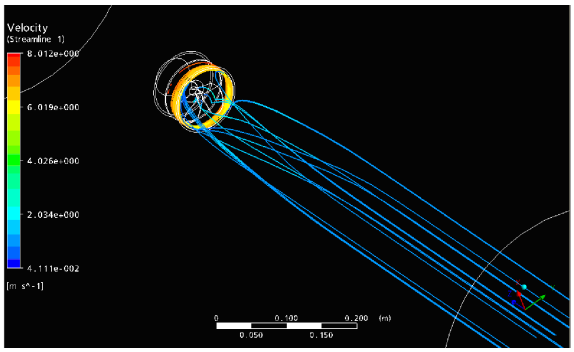

Figure 14. Pathlines

RESULTS

The first scenario considered steady state conditions and an angular velocity of 168 rad/s (which correspond to the motor's maximum speed). Figure 10 shows one of the convergence curves generated by the SOLVER. Figures 11, 12, 13, and 14 are some of the graphs generated in the post-processing stage. Table 4 shows values of the monitored variables.

The second scenario was made in transitory state, with the same velocity as the last case. The results of the steady state

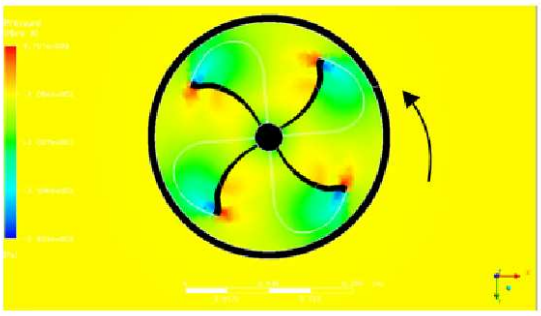

Figure 15. Frontal plane pressure distribution in the place of action of the propeller

Variable	Value
Thrust	10.5813 N
Torque	0.162974 Nm
Power	27.3796 W
J	0.420696
K_Q (Torque)	0.0400913
K_T (Thrust)	0.231406
Efficiency	0.386468

Table 4. Results of the monitored variables - steady state

were used as initial values. The timesteps calculation was made as next:

$$\text{timesteps} = \frac{1\ [\text{rad}]}{168\ [\text{rad s}^{-1}]}\frac{1}{57.29^{\circ}} \approx 0.0001\ [\text{s}]$$

per degree.
Then, to make a complete (360°) turn, the total time would be:

$$\text{total time} = 0.0001 \cdot 360^{\circ} \approx 0.04\ [\text{s}]$$

Figure 16 is one of the convergence curves generated by the SOLVER.
The graphs generated in the post processing stage were similar to the steady state ones (figures 17 and 18). Table 5 shows the values of the monitored variables.

RESULTS ANALYSIS

The w velocity profile graph (figure 11) shows how the upstream flow of the propeller, that has an approximate velocity

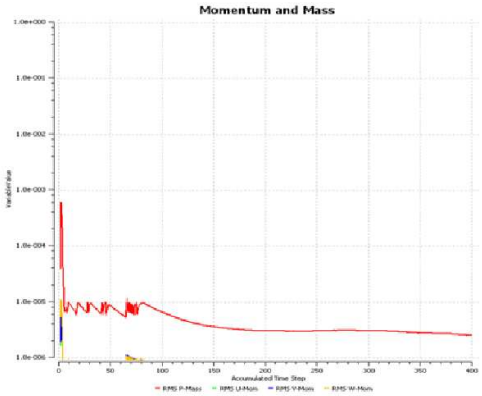

Figure 16. Momentum and mass (transitory)

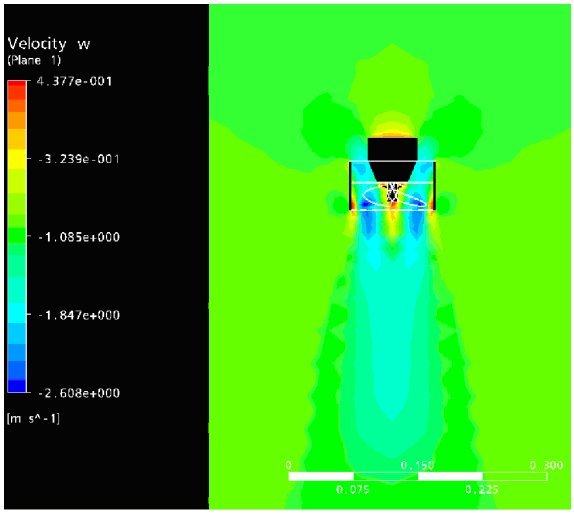

Figure 17. Velocity *w* profile (transitory)

of -1 m/s, accelerates the downstream flow and leaves it with a velocity of -2,592 m/s. The angle of inclination of the motor pointed to the zone of transition of the figure 19, it helps to the separation of the boundary layer, so the flow enters uniform to the zone of action of the propeller, avoiding that it is generated vortexes, upstream. It should also be avoided to have a strangulation of the flow in this zone, because due to the suction action of the propeller and effects of the friction, it could be made of additional forces, taking to the formation of vortexes in this point.

Figure 15 shows a frontal view of the pressure distribution and the action zone of the propeller, were it can be observed the pressure gradient of the leading edge, that has a high pressure zone compared with the trailing edge. This zone of the propeller must have a bigger mechanical resistance, due to the stresses generated. Also, in the tip of the propeller, due to this pressure gradients, vortices that affect propeller's efficiency would be formed. The proximity of the knort nozzle to the tip of the

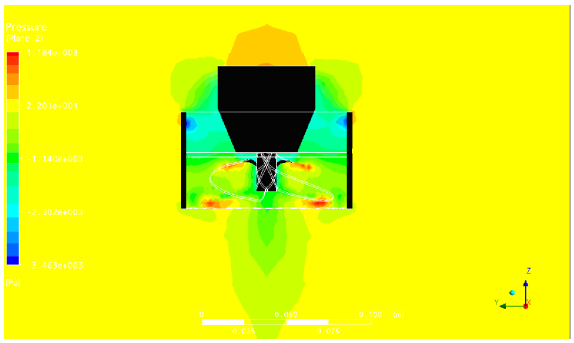

Figure 18. Pressure distribution (transitory)

Variable	Value
Thrust	10.3061 N
Torque	0.159568 Nm
Power	26.8074 W
J	0.420696
K_Q (Torque)	0.0392534
K_T (Thrust)	0.225387
Efficiency	0.384451

Table 5. Results of the monitored variables (transitory)

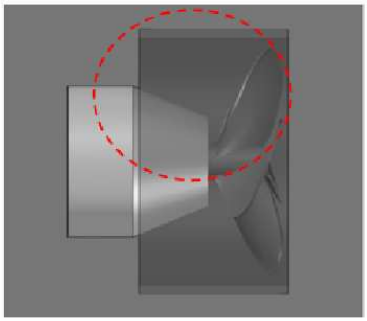

Figure 19. Narrowing zone (Venturi effect)

propeller would reduce this effect.

After running the simulation, the following values of torque and power were obtained:

- Torque: 0.162974 Nm
- Power: 27.3796 W

The results obtained with the CFX tool serve like base to predict the power to move the ROV and to generate the necessary thrust to ovecome the drag forces that it will be subjected. This

information serves like reference to determine the motor to use. It is also necessary to make experimental tests to validate the results obtained with the computational tools. Although these tests are outside of the reach of this study, it propose an assembly for the test to determine the thrust and the necessary power with the selected propeller.See figures 20 and 21.

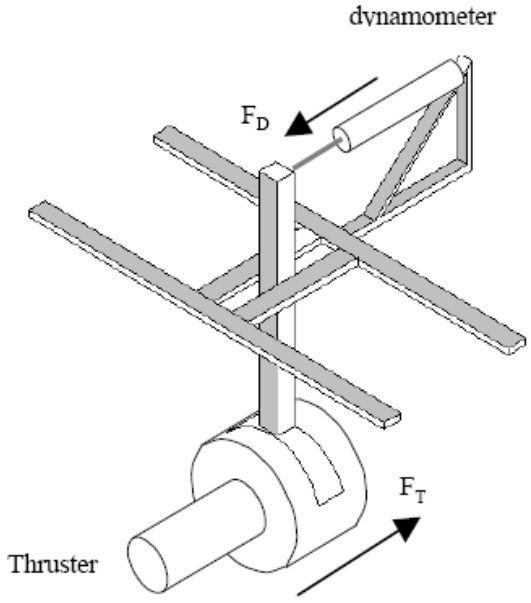

Figure 20. Proposed assembly for the test to determine the thrust and power

Figure 21. Photos of the assembly

It is important to remember that there is a power loss in the system; therefore, the power given by the electrical motor will be bigger than the power transmitted to the propeller, due to losses in the reducer, the bearings, and even in the fluid entering the propeller.

The propeller converts, as efficiently as possible, the power generated by the motor, but as it was mentioned earlier, power transmission involves different steps in which power loss is produced (Figure 22).

The effective power (EHP) is the product between drag and velocity of the submersible expressed in terms of horse power.

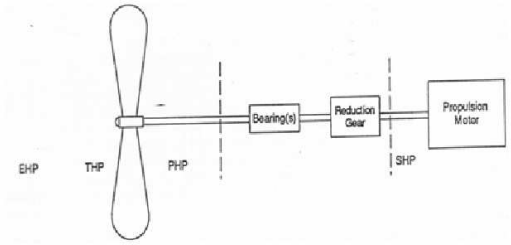

Figure 22. Propulsion System Efficiency. :x Source: ANDERSON, E. Submersible Vehicle Systems Design. Jersey city: The society of naval architects and marine engineer, 1990. 254 p.

$$EHP = \frac{R_T V}{550} \tag{15}$$

The thrust power (THP) is the product between the power that comes from the propeller and the velocity of the submersible expressed in horse power. The difference between THP and EHP is due to two factors: the first one is the drag factor generated by the propeller. The second factor is energy loss because of the flow, which happens in the rear part of the vehicle before it enters into the propeller.

The propulsion power (PHP) is the power delivered to the propeller (the power in the propeller shaft). The difference between PHP and THP is due to the loss in the propellers.

The power delivered by the propeller can be determined as follows:

$$PHP = \frac{2\pi nQ}{550} \tag{16}$$

Where n is the rotation of the motor in rev/s and Q is the torque in lb-ft. The efficiency of the propeller ν_p is defined as:

$$\nu_p = \frac{THP}{PHP} = \frac{TV_A}{2\pi nQ} \tag{17}$$

The axis power (SHP) is given by the propulsion device (electrical or hydraulic motor) towards the axis of the propeller. The difference between SHP and PHP is due to the loss of friction in bearings and gears. Usually in submarines, gears are not used since they increase vehicle's weight and generate loss of power. The efficiency of the machinery n_M is defined as:

$$n_M = \frac{PHP}{SHP} = \frac{Q}{Q_S} \tag{18}$$

Where Q_S is the torque in the propulsion device in lb-ft. Depending on the length of the axis and on the number of bearings, n_M varies between 0.95 up to 0.99.
All the previously defined losses can be combined in a term known as the propulsive coefficient (P_C)

$$\mathrm{P_C} = \frac{\mathrm{EHP}}{\mathrm{SHP}} \tag{19}$$

If this coefficient is big, the efficiency of the propulsion system is bigger and the size of the required power supply is smaller.

All the factors given previously must be considered in the selection process of the propulsion system, this guarantees an appropriate motion of the ROV. The power loss calculations were not performed in this work since many drag values are not known.

CONCLUSIONS

When the mesh is being generated it has to be considered that making a better refinement in the surface of the propeller blade and the rotating zone around it, makes possible to observe with more detail, the distribution of pressures and speeds generated in the tip of the propeller and to see if the formation of vortices occurs.
For the validation of the computational results, it is necessary to apply experimental tests where the experimental thrust generated by the propeller can be measured and, also, to compare it with the results from ANSYS CFX. Likewise, it is necessary to validate computational results, and search into the family of Wageningen B-series propellers, based in the pitch ratio and diameter (P/D), the number of blades and the relation of advance (J), a propeller whose experimental K_T and K_Q can be compared with the values calculated with the program. This validation would apply the momentum and blade element theory for evaluate the propeller selected.

It is appropriate, before selecting the motors, to calculate friction losses that occur throughout the transmission system, to guarantee the necessary operational torque.

REFERENCES

[1] ROVEXCHANGE, 2006. Rov specifications & reviews. [online] http://www.rovexchange.com.

[2] Meadows, G. and Meadows, L, 2003. *Ship design and construction*, lamb, t. ed., Vol. 1. The society of naval architects and marine engineers, Jersey City (NJ), ch. The marine environment, pp. 1 – 16.

[3] Allmendinger, E., 1990. *Submersible vehicle systems design*. The society of naval architects and marine engineers, Jersey City (NJ).

[4] Griffiths, G., 2003. *Technology and applications of autonomous underwater vehicles*. Taylor & Francis, London.

[5] Bohm, H., and Jensen, V. *Introduction to underwater technology and vehicle design*. Marine Advanced Technology Education (MATE), Monterrey Peninsula College.

[6] Rhee, S., and Joshi, S., 2005. "Computational validation for flow around a marine propeller using unstructured mesh based navier-stokes solver". *JSME International Journal*, **48**(3).

[7] MEGSC-2006-CONFERENCE-PROCEEDINGS, 2006. Simulation of the flow past a marine propeller under design and off-design conditions, 4th annual conference of the Computational Fluid Dynamics Society of Canada.

[8] Bernitsas, M., Ray, D., and Kinley, P., 1981. Kt, kq and efficiency curves for the wageningen b-series propellers. Tech. rep., Department of Naval Architecture and Marine Engineering, Michigan.

[9] Vysohlid, M., and Mahesh, K., 2004. "Large eddy simulation of propeller crashback".